

Neuroblastoma chemotherapy can be augmented by immunotargeting O-acetyl-GD2 tumor-associated ganglioside

S. Faraj, M. Bahri, S. Fougeray, A. El Roz, J. Fleurence, J. Véziers, M. D. Leclair, E. Thébaud, F. Paris & S. Birklé

To cite this article: S. Faraj, M. Bahri, S. Fougeray, A. El Roz, J. Fleurence, J. Véziers, M. D. Leclair, E. Thébaud, F. Paris & S. Birklé (2018) Neuroblastoma chemotherapy can be augmented by immunotargeting O-acetyl-GD2 tumor-associated ganglioside, *Oncolmmunology*, 7:1, e1373232, DOI: [10.1080/2162402X.2017.1373232](https://doi.org/10.1080/2162402X.2017.1373232)

To link to this article: <https://doi.org/10.1080/2162402X.2017.1373232>

 View supplementary material [↗](#)

 Accepted author version posted online: 01 Sep 2017.
Published online: 21 Sep 2017.

 Submit your article to this journal [↗](#)

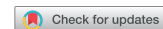
 Article views: 443

 View related articles [↗](#)

 View Crossmark data [↗](#)

 Citing articles: 3 View citing articles [↗](#)

ORIGINAL RESEARCH



Neuroblastoma chemotherapy can be augmented by immunotargeting O-acetyl-GD2 tumor-associated ganglioside

S. Faraj^{a,b,†}, M. Bahri^{a,†}, S. Fougeray^{a,c,‡}, A. El Roz^{a,c,‡,§}, J. Fleurence^{a,c}, J. Véziers^d, M. D. Leclair^{b,e}, E. Thébaud^f, F. Paris^a, and S. Birklé ^{a,c}

^aCRCINA, INSERM, Université d'Angers, Université de Nantes, Nantes, Loire Atlantique, France; ^bService de chirurgie pédiatrique, CHU de Nantes, 38 boulevard Jean Monnet, Nantes, Loire Atlantique, France; ^cUniversité de Nantes, UFR des Sciences Pharmaceutiques et Biologiques, 9 rue Bias, Nantes, Loire Atlantique, France; ^dINSERM, UMRS 1229, RMeS "Regenerative Medicine and Skeleton", CHU Nantes, PH4 OTONN, Université de Nantes, UFR Odontologie, SC3M Plateform, UMS INSERM 016 – CNRS 3556, SFR François Bonamy, 1 place Alexis Ricordeau, Nantes, Loire Atlantique, France; ^eUniversité de Nantes, UFR de Médecine, 1 rue Gaston Veil, Nantes, Loire Atlantique, France; ^fService d'oncologie pédiatrique, CHU de Nantes, quai Moncoussu, Nantes, Loire Atlantique, France

ABSTRACT

Despite recent advances in high-risk neuroblastoma therapy, the prognosis for patients remains poor. In addition, many patients suffer from complications related to available therapies that are highly detrimental to their quality of life. New treatment modalities are, thus, urgently needed to further improve the efficacy and reduce the toxicity of existing therapies. Since antibodies specific for O-acetyl GD2 ganglioside display pro-apoptotic activity against neuroblastoma cells, we hypothesized that combination of immunotherapy could enhance tumor efficacy of neuroblastoma chemotherapy.

We demonstrate here that combination of anti-O-acetyl GD2 monoclonal antibody 8B6 with topotecan synergistically inhibited neuroblastoma cell proliferation, as shown by the combination index values. Mechanistically, we evidence that mAb 8B6 induced plasma cell membrane lesions, consistent with oncosis. Neuroblastoma tumour cells treated with mAb 8B6 indeed showed an increased uptake of topotecan by the tumor cells and a more profound tumor cell death evidenced by increased caspase-3 activation. We also found that the combination with topotecan plus monoclonal antibody 8B6 showed a more potent anti-tumor efficacy *in vivo* than either agent alone. Importantly, we used low-doses of topotecan with no noticeable side effect. Our data suggest that chemo-immunotherapy combinations may improve the clinical efficacy and safety profile of current chemotherapeutic modalities of neuroblastoma.

ARTICLE HISTORY

Received 6 March 2017
Revised 25 August 2017
Accepted 25 August 2017

KEYWORDS

Neuroblastoma;
Chemoimmunotherapy;
O-Acetyl-GD2; Therapeutic
Antibody; Topotecan

Introduction

Neuroblastoma (NB) is a cancer of the sympathetic nervous system derived from primordial neural crest cells.¹ It is characterized by a highly heterogeneous clinical behavior, ranging from spontaneous regression to rapid progression and patient death. High-risk NB occurs in half of all patients and is associated with metastasis, amplification of the MYCN oncogene, and an unfavorable prognosis.² Despite intensive multi-modal treatment, recent developments in immunotherapy and inclusion of novel targeted drugs in clinical trials, the prognosis of children with high-risk neuroblastoma is still poor, with a median 5-year overall survival between 50 and 70%.^{3,4} Moreover, available therapies remain highly detrimental to patients' quality of life.⁵⁻⁷ For example, the anti-GD2 therapeutic antibody dinutuximab often causes dose-limiting side effects, such as severe pain during and after the infusion.⁸ This on-target toxicity is related to the expression of GD2 on normal tissues such as peripheral nerve fibers.⁹ In addition, many patients

with chemo-sensitive disease who survive suffer from substantial therapy-related toxicities that result in poor long-term health outcomes for survivors.⁵⁻⁷ There is thus an urgent need to further improve the efficacy and lessen the toxicities of neuroblastoma therapies.

Our group focuses on immunotherapeutic strategies targeting the O-acetylated form of GD2 (OAcGD2), which we believed could reduce the acute toxicities currently associated with anti-GD2 therapeutic antibodies. Significantly, anti-OAcGD2 antibodies do not bind to peripheral nerves unlike anti-GD2 therapeutic antibodies.¹⁰ In addition, mAbs specific for OAcGD2 do not induce pain sensitization in rats contrast to dinutuximab while presenting potent anti-neuroblastoma activity *in vivo*.¹¹ The mechanisms by which anti-OAcGD2 mAbs induce tumor regression *in vivo* are thought to involve complement-dependent cytotoxicity (CDC), antibody-dependent cell cytotoxicity (ADCC), and induction of a programmed

CONTACT S. Birklé  Stephane.Birkle@univ-nantes.fr

 Supplemental data for this article can be accessed on the [publisher's website](#).

[†]These are first co-authors.

[‡]These are second co-authors.

[§]Present address: Faculty of Public Health, Lebanese German University, Sahel Alma Highway, P.O. Box 206, Jounieh, Lebanon.

cell death with attributes of apoptosis.^{11,12} Interestingly, this latter property could be applied to enhance the susceptibility of neuroblastoma cells to cytotoxic anti-cancer drugs for a better control of disease while reducing chemotherapy dosage and side effects.

Here we investigated whether the anti-OAcGD2 mAb 8B6 could serve as a sensitizing agent against neuroblastoma cells. For this purpose, we tested topotecan, a topoisomerase I inhibitor, used in the treatment of neuroblastoma.¹³ The objective of the study was to delineate the mechanism(s) by which mAb 8B6 could sensitize neuroblastoma cells against cytotoxic drugs since this may lead to rational development of therapeutic clinical trials.

Results

Treatment with topotecan does not affect OAcGD2 expression on neuroblastoma cells

Previous studies showed that GD2 expression—the precursor of OAcGD2—can be altered in neuroblastoma cells upon exposure to chemotherapeutic drugs.^{14,15} Thus, we first tested if exposure to topotecan would affect the expression level of anti-OAcGD2 in neuroblastoma cells. To this end, we treated tumor cells with topotecan for 48 hours before studying OAcGD2-expression by flow cytometry analysis, as described in Material and Methods Section. As shown in Fig. 1A, the level of mAb 8B6 binding on either NXS2, IMR5, LAN1, or LAN5 cells remained mostly unchanged after 48-hour incubation with topotecan. We also evaluated OAcGD2 expression after topotecan chemotherapy *in vivo* using the NXS2 mouse neuroblastoma experimental liver metastasis model. After NXS2 cells injection, mice were treated with topotecan as described in the Material and Methods section. Twenty-eight days after tumor cells inoculation, we collected NXS2 liver metastasis samples for OAcGD2 expression analysis. Using an immunoperoxidase assay performed with biotinylated-8B6 mAb specific for OAcGD2, we found that biotinylated-8B6 mAb stained NXS2-tumor sections similarly in mice treated with topotecan (Fig. 1B). The isotype-matched irrelevant antibody was negative (Fig. 1B). Similar observations were found in human IMR5 neuroblastoma xenografts (Fig. S1). Taken together these results show that topotecan treatment does not affect mAb 8B6 binding level on tumor cells, and suggest mAb 8B6 may be used in combination with chemotherapeutic drugs against NB cells.

Anti-OAcGD2 mAb 8B6 synergistically enhances the inhibitory effects of topotecan on neuroblastoma cell lines

To test whether mAb 8B6 could enhance topotecan chemotherapy, we next characterized the effects on tumor cell viability of mAb 8B6 in combination with topotecan in four different neuroblastoma cell lines, using an MTT assay. First, exposing of NXS2, IMR5, LAN1, or LAN5 cells to topotecan alone resulted in a concentration-dependent inhibition of cell viability (Fig. 2A). Next, we combined topotecan in six combinational equipotent ratios based on the ED₅₀ values in order to assess effect on cell viability and obtain the combination index values by the method of Chou and Talalay.¹⁶ Addition of mAb 8B6 enhanced the

anti-proliferative effect of topotecan in each studied cell line. As shown in Fig. 2, the combination dose-response curves shifted towards sensitive side of the graph indicating that combination of mAb 8B6 with topotecan was more efficient in inhibiting neuroblastoma cell viability. Moreover, the calculated ED₅₀ values of topotecan were significantly lower in the presence of mAb 8B6 ($p < 0.05$, Table 1). Finally, we calculated the combination index (CI) values to characterize the effects of the combination tested (Fig. 2B). We found that median combination index values were significantly less than 1.0 ($p < 0.05$), indicating a synergistic interaction (Fig. 2). We observed the strongest synergy in IMR5 cells with CI values < 0.5 . Similarly, synergy was attained in LAN1 cells (CI values: 0.4-0.6). In NXS2 and LAN5 cells synergy was observed at ED₅₀ and ED₇₅ (CI values: 0.4-0.8), while an additive effect was attained at ED₉₀ with CI values of approximately 1. We concluded that mAb 8B6 has the potential as an adjuvant therapeutic agent, enabling use of lower doses of topotecan in current clinical use.

Increased-topotecan sensitivity induced by anti-OAcGD2 mAb 8B6 involves loss of membrane integrity

We went on to investigate the mechanism by which mAb 8B6 sensitizes neuroblastoma cells to topotecan. It was proven that anti-ganglioside mAbs could induce an alternative form of programmed cell death through oncosis.^{17,18} Features of oncosis include cell swelling, membrane damage associated with increased cell permeability, and cell death.¹⁹⁻²¹ In our previous work, we observed under light microscopy that tumor cells treated with mAb 8B6 aggregated and underwent morphologic changes, which was followed by cell death.¹² Based on this evidence, we investigated here an oncosis-like mechanism as the probable mAb 8B6 mode of action in tumor cell sensitization to topotecan. Thus, we examined the cell surface of neuroblastoma cells for structural changes after mAb treatment with scanning electron microscopy (Fig. 3). Strikingly, neuroblastoma cell plasma membranes displayed numerous pores in the presence of anti-OAcGD2 mAb 8B6 (Fig. 3). These effects were not seen when the cell were treated with the control antibody (Fig. 3). Next, we carried out a flow cytometry assay to study topotecan incorporation in the mAb-treated cells. Remarkably, the analysis of MFI ratios of intracellular topotecan fluorescence indicated that topotecan uptake was significantly greater in the mAb 8B6-treated neuroblastoma cells than in the control cells (Fig. 4A, and Fig. S2). Taken together, these data indicate that mAb 8B6-treated cells display cell membrane injuries that result in increased cell permeability to topotecan. In parallel, we conducted immunoblots analysis to study the cleaved caspase-3 level in the tumor cells treated with both mAb 8B6 and topotecan (Fig. 4B). As shown in Fig. 4B, the increased intracellular topotecan uptake induced by mAb 8B6 correlated with a gain of cleaved caspase-3 level in all studied neuroblastoma cell lines, indicating a more profound cell death. These findings suggest that alteration of the tumor cell plasma membrane permeability as a mechanism for the synergism between mAb 8B6 and topotecan combination.

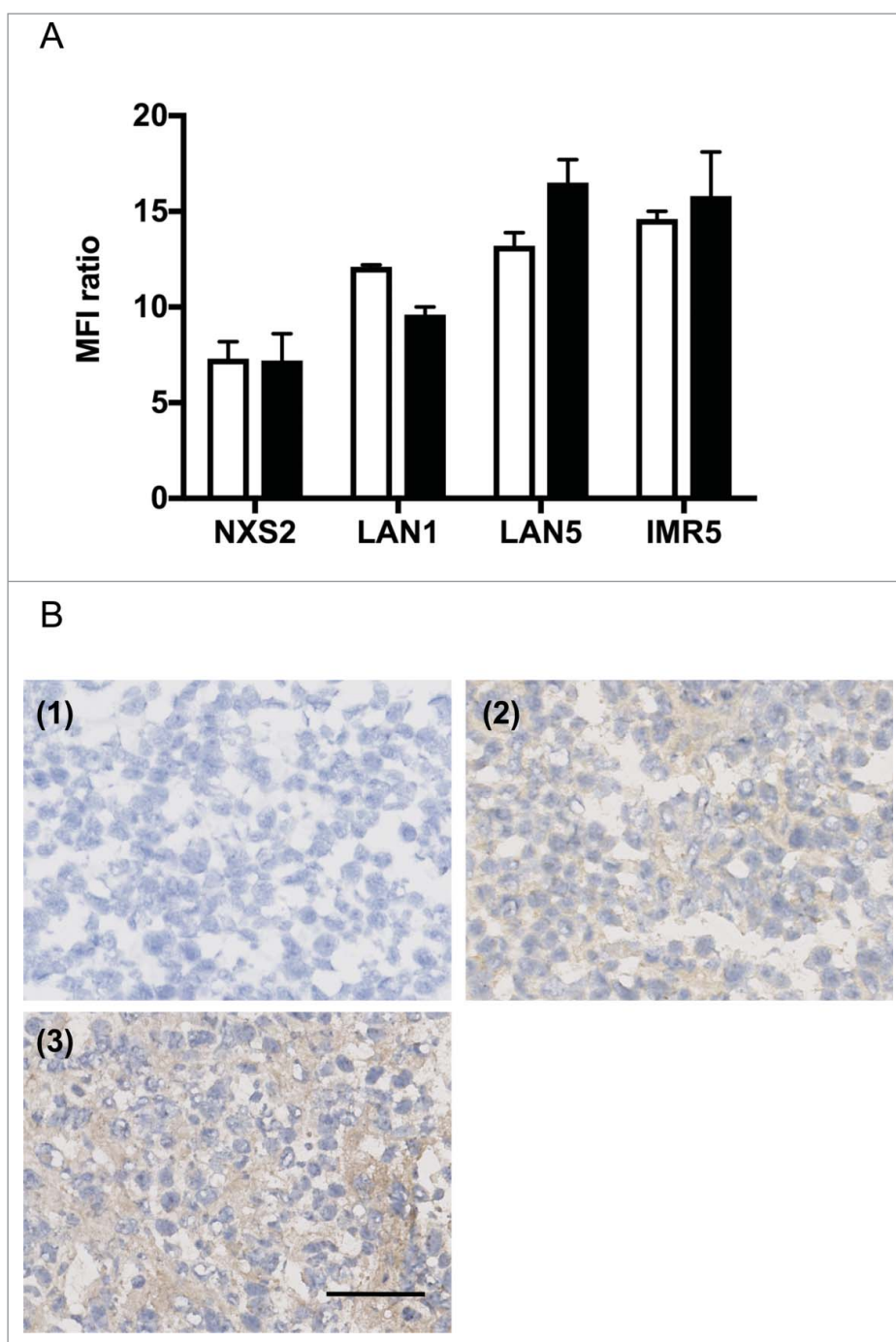


Figure 1. Exposure to topotecan does not affect OAcGD2 expression in neuroblastoma cells. (A) Binding activity of anti-OAcGD2 mAb 8B6 on NXS2, LAN1, LAN5, and IMR5 neuroblastoma cell lines as indicated, before (empty column) and 48 hours (black column) after incubation with topotecan. The geometric mean fluorescence intensities (MFIs) of tumor cells stained with mAb 8B6 were normalized to the MFIs of tumor cells stained with the isotype-control antibody. Results are presented as mean \pm SEM (n = 3, independent experiments) of MFI ratios as described in the material and methods. (B) Representative NXS2 liver metastasis section stained with biotinylated-8B6 mAb using an immunoperoxidase assay of either vehicle-treated mice (2) or topotecan-treated mice (3). Tumors were collected on day 28 after NXS2 cells inoculation and topotecan chemotherapy was performed as described in the Material and Methods section. Strong immunostaining with biotinylated-8B6 mAb was observed on neuroblastoma cells in each treatment regimens. The control biotinylated-antibody was used as a negative control (1). Three NXS2 tumors from 3 different mice in each experimental group were tested with the same result. Scale bar = 100 μ m.

Anti-OAcGD2 mAb 8B6 enhances anti-tumor activity of topotecan in vivo

To extend our observations obtained *in vitro*, we next evaluated the potential therapeutic effects of the combination of mAb 8B6 and topotecan combination *in vivo*. We performed the *in vivo* studies using the mouse NXS2 neuroblastoma

experimental liver metastasis that we previously used to evaluate the anti-tumor activity of mAb 8B6 as a single agent.^{10,11} Topotecan was given at low doses as previously reported in the literature to minimize related side effects.^{22–24} Three day after i.v. NSX2 tumor cells inoculation, ten mice were assigned to treatment with single agent, or combination of mAb 8B6 and

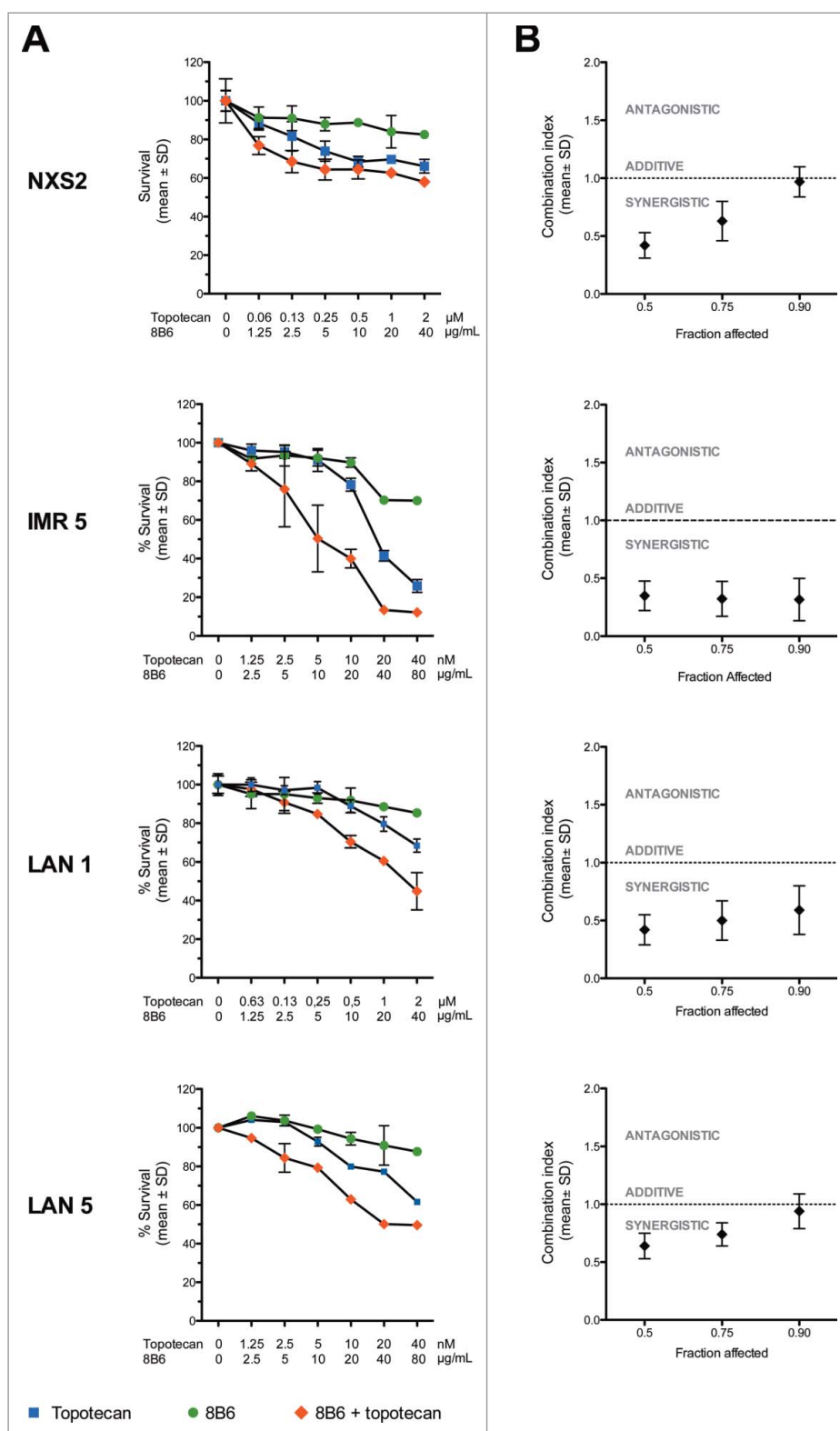


Figure 2. Anti-OAcGD2 mAb 8B6 synergizes with topotecan *in vitro*. The neuroblastoma cell lines IMR5, LAN1, LAN5, and NXS2 were treated either singly, or with combination of topotecan and mAb 8B6, as indicated, and the MTT viability assay was carried out after 72 hours. (A) Dose-response curves and (B) combination index plots. Dose-response curves shown are representative of three independent replicates. Percentage survival values were transformed into Fraction affected (Fa) values and used to calculate combination index (measure of synergy, additivity and antagonism) using Compusyn software. In the combination index plots, data are presented as mean \pm SEM for three independent replicates. Results showed that mAb 8B6 had a synergistic effect with topotecan (CI < 1).

chemotherapeutic drug (Fig. 5A). On day 28 after tumor cells inoculation, we determined the liver weight after mice euthanasia. The dose of mAb 8B6 (cumulative dose = 150 μ g) that we used in this study yielded a significant reduction of NXS2 liver

metastasis, as indicated by the liver weight, compared to the vehicle treated mice. The mean liver weight in mAb 8B6-treated group was 1.5 \pm 0.15 g compared to 2.5 \pm 0.18 g for the vehicle-treated group ($p < 0.05$, Fig. 5B). The specificity of mAb 8B6

Table 1. Characterization of neuroblastoma cell lines and ED₅₀ of topotecan used as a single agent or in combination with mAb 8B6.

Cell line	MYCN Amplification	ED ₅₀ of topotecan(μM) ^a		p value
		Without mAb 8B6	With mAb 8B6	
NXS2	No ⁵³	4.7 ± 0.3	1.2 ± 0.15	< 0.01
IMR5	Yes ⁵⁴	0.010 ± 0.001	0.005 ± 0.001	< 0.01
LAN1	Yes ⁵⁵	7.5 ± 1.2	1.9 ± 0.2	< 0.01
LAN5	Yes ⁵⁶	0.024 ± 0.007	0.005 ± 0.001	< 0.01

^aED₅₀ were calculated using CompuSyn software as described in the Material and Methods Section. Data represent the mean of 3 independent experiments ± SEM.

^bAnti-OAcGD2 mAb 8B6 was combined with topotecan at the concentration of 40 μg/ml.

therapy was demonstrated, since treatment with an equivalent amount of non-specific antibody was completely ineffective (mean liver weight = 2.4 ± 0.17 g, $p > 0.05$ compared to vehicle-treated mice, Fig. 5B). The combination of topotecan (0.36 mg/kg, i.p., five times weekly for 1 week) plus mAb 8B6 significantly reduced liver weight (0.9 ± 0.03 g) compared to either topotecan (1.22 ± 0.09 g), or mAb 8B6 used as single agent ($p < 0.05$, Fig. 5B).

Weight loss is used as a sensitive marker for health monitoring.²⁵ We therefore performed a parallel analysis of the body weight over the treatment period. We observed no loss of body weight, suggesting no treatment-related toxicity in the mice treated with mAb 8B6, topotecan, or topotecan + mAb 8B6 (Fig. 5C).

To exclude any topotecan-induced immunomodulatory effect that may enhance anti-tumor activity of mAb 8B6 *in vivo*, we further studied the therapeutic performance of the combination regimen in severe immunodeficient NGS mice bearing subcutaneous IMR5 tumors. Therapy started 7 days after subcutaneous injection of IMR5 cells, when tumors had reached an average size of 50 ± 2.5 mm³ (Fig. 6A). Mice were treated with either mAb 8B6 (150 μg, i.v., day 7 and day 11), topotecan (0.36 mg/kg i.p., day 7–11) or combination of mAb 8B6 and topotecan. We monitored the tumor volume and the health of the mice during the course of the experimentation. The event resulting in mouse euthanasia was disease progression, defined as the tumor volume reaching above 1 cm³. Monotherapy with either mAb 8B6 or topotecan led tumor growth retardation compared with the control groups treated with either vehicle or control antibody (Fig. 6A). This resulted in a substantial improved event-free survival (EFS) of mice treated with either topotecan or mAb 8B6, as single agent, compared to the control mice (median EFS of 21 days for the vehicle-treated group, 22 days for the control antibody-treated group, 26 days for topotecan-treated mice and 29 days for mAb 8B6-treated mice, Fig. 6B). Interestingly, the combination of mAb 8B6 and topotecan significantly delayed tumor growth compared to either mAb or topotecan given alone (Fig. 6A). When we compared the tumor sizes between the monotherapy arms and the combination group, the differences were statistically significant ($p < 0.05$, mAb 8B6 vs. combination therapy; $p < 0.01$, topotecan vs. combination therapy) at different time points (from day 15 to day 26, Fig. 6A). Moreover,

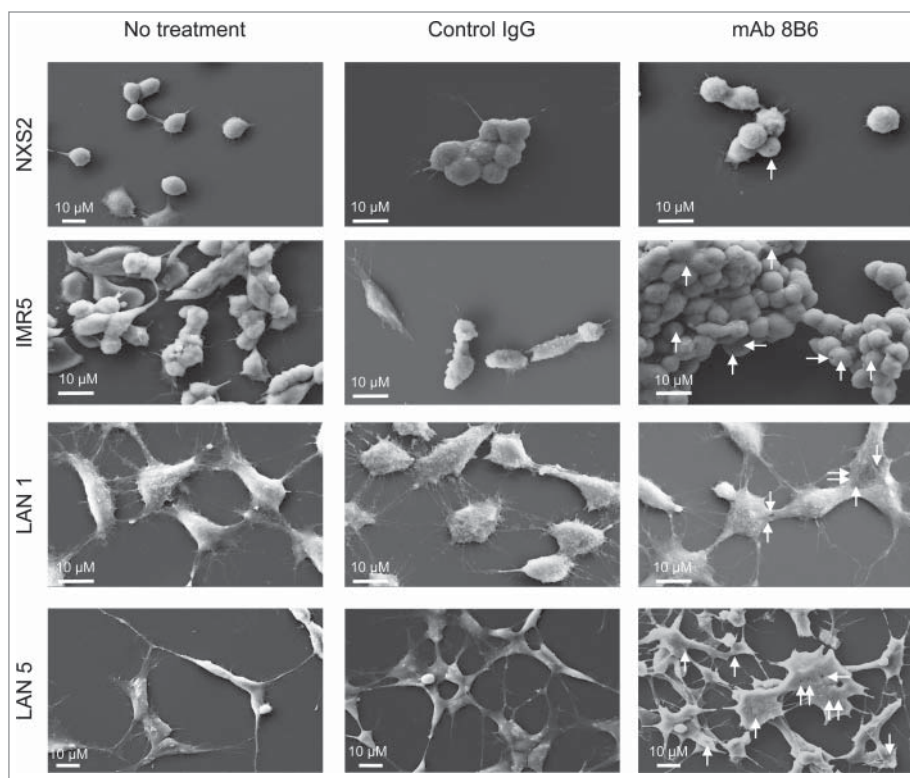


Figure 3. Morphological changes induced by mAb 8B6. Analysis by scanning electron microscopy showed morphological changes in neuroblastoma cells treated with mAb 8B6. NXS2, IMR5, LAN1, and LAN5 neuroblastoma cells were incubated with either control antibody or mAb 8B6 at 37°C for 30 minutes. Electron micrographs were then taken. Membrane pores were seen in all studied neuroblastoma cells treated with mAb 8B6 displayed pores. Similar results were observed in three independent experiments. Membrane lesions are indicated with white arrows. Horizontal rods correspond to the scale bar, as indicated.

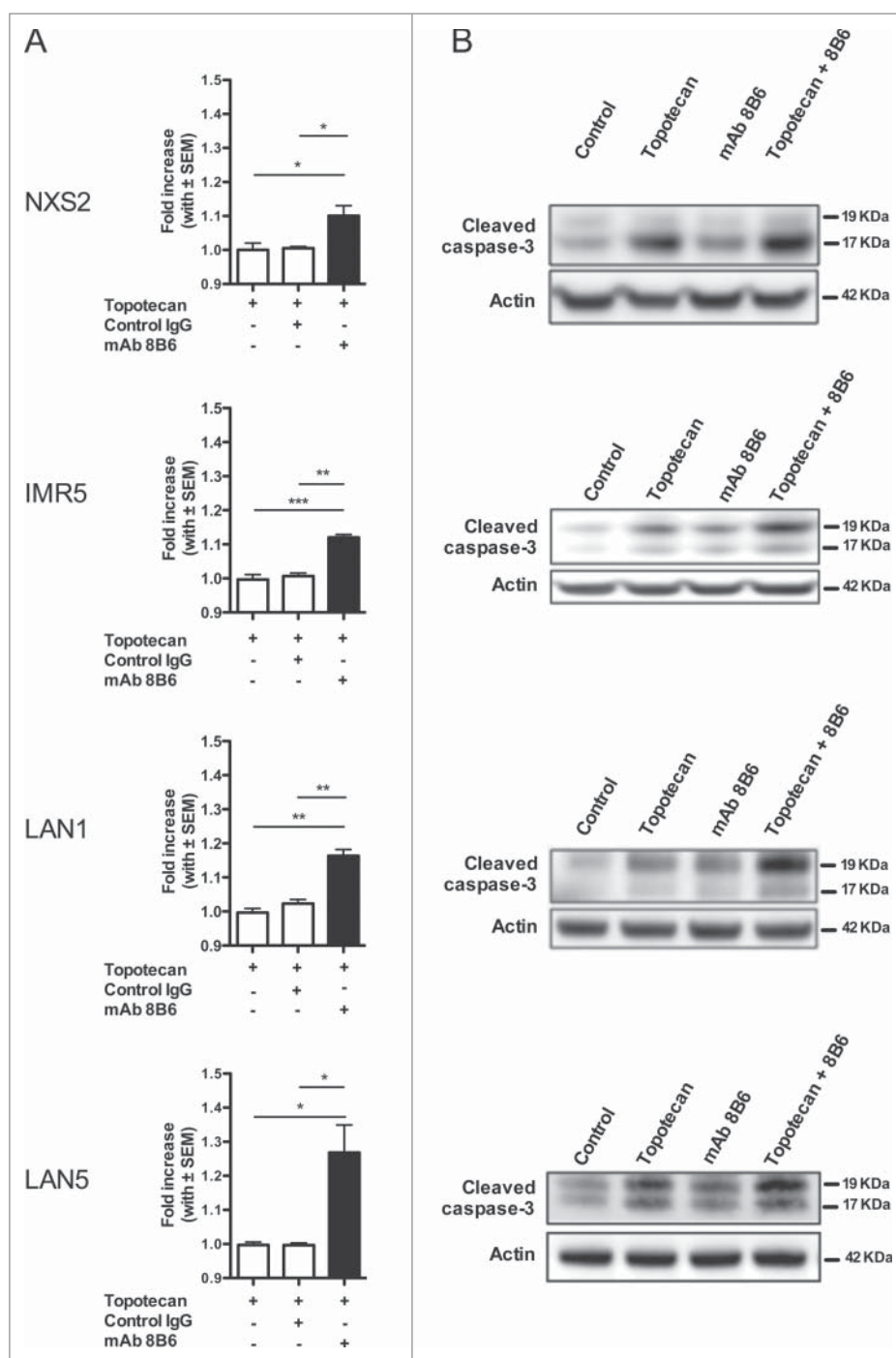


Figure 4. Anti-OAcGD2 mAb causes an increase in the plasma membrane topotecan permeability followed by a gain of topotecan-induced caspase-3 activation. (A) NXS2, IMR5, LAN1, and LAN5 neuroblastoma cells were incubated with topotecan in the presence of either mAb 8B6 or control IgG for 30 minutes. After incubation, intracellular fluorescence of topotecan was analyzed by flow cytometry. The geometric mean fluorescence intensities (MFIs) of the different experimental conditions were normalized to the MFIs of tumor cells incubated with topotecan alone. A gain of topotecan uptake was seen in all neuroblastoma cell incubated with mAb 8B6 + topotecan, as indicated. (B) The cells in (A) were also assessed by Western blot analysis for caspase-3 activation detection. The right panels show representative images of immunoblots of cleaved caspase-3. Elevated level of cleaved caspase-3 was seen in all neuroblastoma cells treated with mAb 8B6 + topotecan, as indicated. Similar results were observed in three independent experiments. Data presented are mean \pm SEM of triplicate experiments. * $p < 0.05$, ** $p < 0.01$, *** $p < 0.001$.

treatment with combination of mAb 8B6 and topotecan had the greatest impact on animal survival with a median EFS of 39.5 days ($p < 0.05$, mAb 8B6 vs. combination therapy; $p < 0.01$, topotecan vs. combination therapy, Fig. 6B). No significant weight loss was observed in mice treated with topotecan or mAb 8B6 alone or in combination throughout the course of the study (Fig. 6C). These observations suggest that the combination with low-schedule topotecan plus mAb 8B6 presents a more potent

anti-tumor efficacy *in vivo* than either agent alone, without detectable toxicity.

Discussion

Given the tissue distribution pattern of OAcGD2, specific mAbs provide a potential opportunity to develop safer immunotherapeutic strategies than anti-GD2 therapeutic

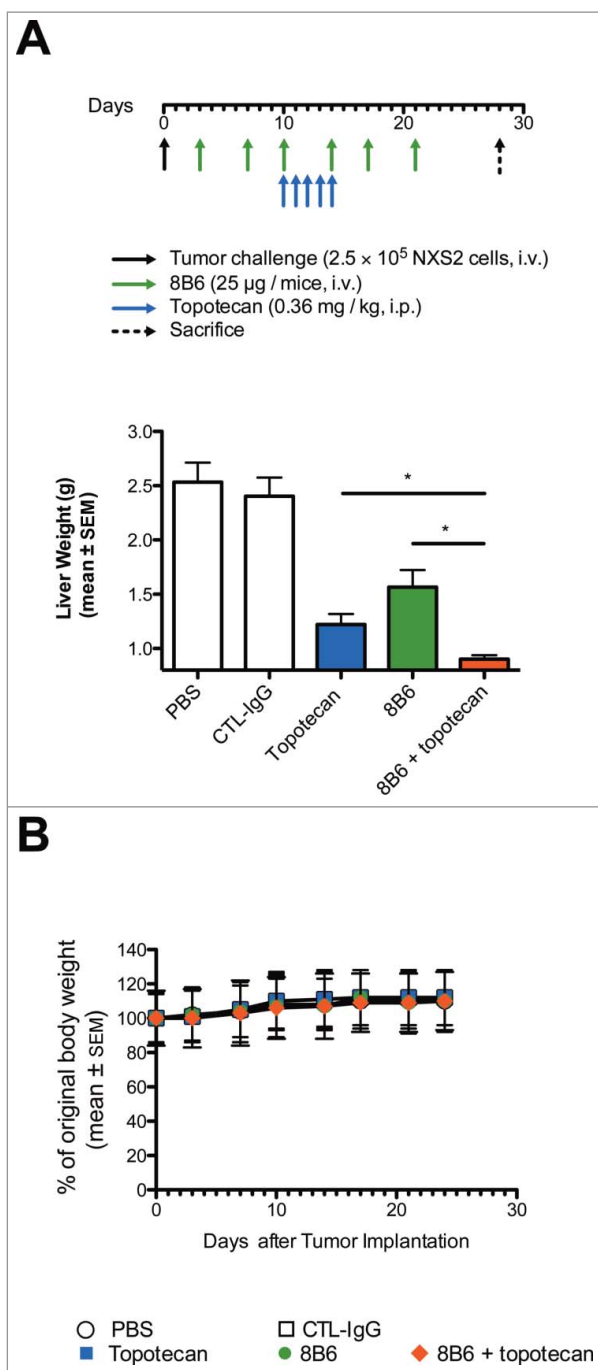


Figure 5. Enhancement of topotecan anti-tumor activity in vivo against established experimental liver metastasis by mAb 8B6 specific for O-acetyl-GD2. (A) Mice ($n = 10$ /group) were inoculated with 2.5×10^5 NXS2 cells by i.v. injections. mAb 8B6 treatment was started on day 3 after tumor cell inoculation twice a week for 3 consecutive weeks (cumulative dose = 150 μ g). Topotecan treatment was started at day 10 post-tumor inoculation. Topotecan was given by i.p. injections at 0.36 mg/kg five times weekly for 1 week. Mice were euthanized 28 days post-tumor inoculation. (B) Anti-tumor efficacy was evaluated by determining the liver weight on the fresh specimen. The y-axis starts at 0.8 g corresponding to the average of normal liver weight. (C) Mean weight for each treatment group, as indicated. Mean weight of mice at day 0 was defined as 100% weight. Weight in each group remained stable for the period of treatment. Data are presented as the mean \pm SEM. * $p < 0.05$.

antibodies.¹⁰ Taking into consideration that anti-OAcGD2 mAb 8B6 promotes tumor cell death without the involvement of the immune system,¹² we examined here the effect of anti-OAcGD2 mAb in combination with topotecan, one clinically

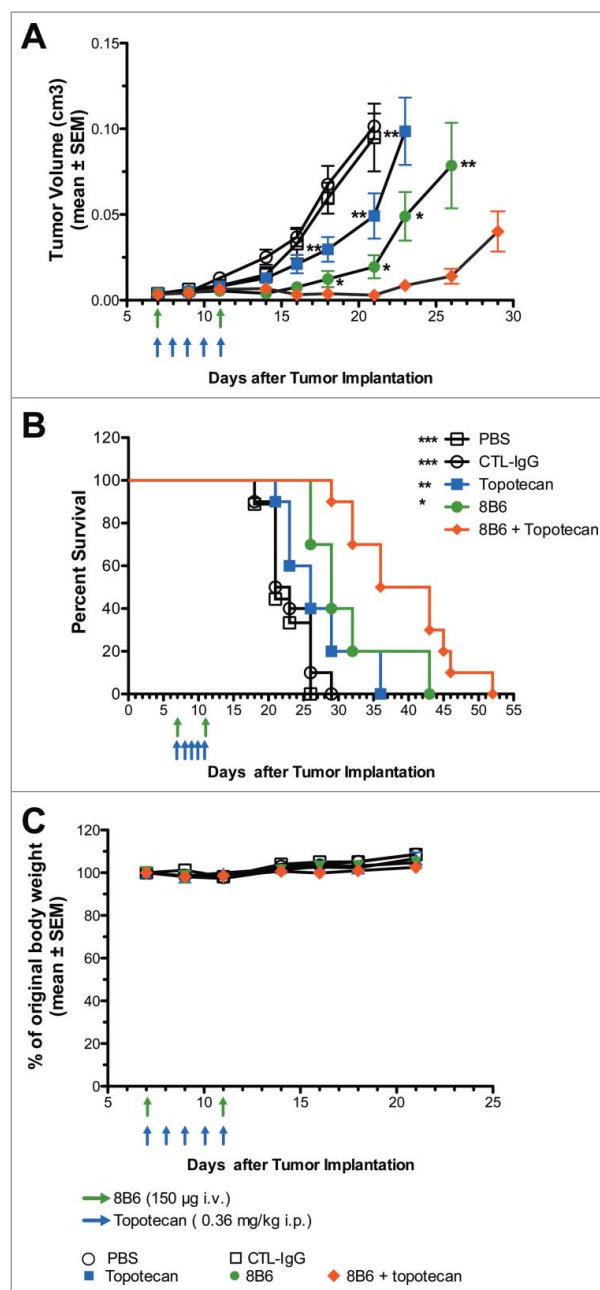


Figure 6. In vivo effect of mAb 8B6 + topotecan on tumor growth and event-free survival in IMR5 xenograft model. NSG mice bearing (A) human neuroblastoma IMR5 xenograft were treated with vehicle (PBS, i.p.), topotecan alone (0.36 mg/kg i.p.), control IgG alone (150 μ g, i.v.), mAb 8B6 alone (i.p.), or topotecan + mAb 8B6, as indicated. Administration of mAb 8B6 or control antibody treatment started on day 7 after IMR5 cells inoculation and was repeated once on day 11. Topotecan or PBS treatment were started on day 7 and given 5 consecutive days. Tumor growth was monitored and tumor volumes were calculated. Mean tumor volume \pm SEM of each treatment group (PBS group, 9 mice; all other groups, 10 mice) are depicted (* $p < 0.05$ for mAb 8B6 against mAb 8B6 + topotecan, ** $p < 0.01$ for topotecan against mAb 8B6 + topotecan, as indicated). (B) Event Free Survival Kaplan-Meier curves were analyzed by log-rank Mantel-Cox test, where $p < 0.5$ was considered significant. The p values reported refer to the combination treatment compared to vehicle / control antibody / topotecan / mAb 8B6. * $p < 0.05$, ** $p < 0.01$, *** $p < 0.001$. (C) Mean weight for each treatment group, as indicated. Mean weight of mice on day 0 was defined as 100% weight. Weight in each group remained stable for the period of treatment. Data are presented as the mean \pm SEM.

relevant chemotherapeutic drug used against neuroblastoma.²⁶ The rationale for combining immune therapies with chemotherapy to improve neuroblastoma patients outcomes is suggested by the finding that anti-GD2 mAb 14G2a sensitizes

neuroblastoma cells to chemotherapeutic agents in killing neuroblastoma cells *in vitro*,²⁷ based on its ability to induce apoptosis in tumor cells.²⁸ Yet, the identification of the mechanisms involved at the cellular level remains necessary to define the best chemotherapeutic agent to be used in such combination. The study of the importance of GD2 in tumor cell apoptosis remains however challenging, partly because anti-GD2 antibodies cross-react with OAcGD2.^{29,30} Despite much effort to elucidate the apoptotic pathways induced by anti-GD2 mAb, few mechanisms have been yet identified to date.³¹ Here, we present findings that delineate a new mechanism of action in which anti-OAcGD2 mAbs induce the loss of tumor cell membrane integrity resulting in an increased cytotoxic drug uptake and a more potent anti-neuroblastoma cytotoxicity. These findings represent a new potential therapeutic application of mAbs specific for OAcGD2 ganglioside for the treatment of patients with neuroblastoma. In particular, we used topotecan, a clinically relevant chemotherapeutic drug.¹³

In view of previous reports that treatment of neuroblastoma cells with drugs is accompanied by a decrease in cell content of GD2,^{14,15} we first analyze the OAcGD2 expression-level upon topotecan treatment. Our data demonstrate that both *in vitro* and *in vivo* exposure of neuroblastoma cells to topotecan does not result in the loss of OAcGD2 expression in these cells. These data provide a strong read out for topotecan combination therapy with anti-OAcGD2 immunotherapy.

Having found that OAcGD2 expression was not affected by topotecan treatment in neuroblastoma cells, we next determined whether the combined treatment would result in a higher cytotoxicity towards neuroblastoma cells. In line with the previous work of Kowalczyk et al.,²⁷ we evidenced that the combination of mAb 8B6 plus topotecan significantly enhanced the anti-neuroblastoma activity of either topotecan or mAb 8B6 alone. We also found that the calculated combination index values at ED₅₀, ED₇₅ and ED₉₀ were < 1, demonstrating a synergistic effect.¹⁶ Of note, we used three human neuroblastoma cell lines with MYCN gene amplification, a genetic factor associated with poor outcome and that is frequently over-expressed in neuroblastoma tumors.³²

Mostly, our findings reveal here a new cell death mechanism by which mAb 8B6 promotes tumor cell chemosensitization. We reported earlier that mAb 8B6 induces tumor growth inhibition *in vitro* with feature of apoptosis, included caspase-3 activation.¹² We also suggested that this activity could contribute significantly to its clinical performance, based on our earlier data obtained in immune compromised mice bearing neuroblastoma xenografts.¹² Our previous observations also showed that the cell death induced by mAb 8B6 was associated with cell swelling, as evidenced by light microscopy.¹² This phenomenon prompted us to investigate the implication of an oncosis-like mechanism, as suggested with anti-glycolyl-GM3 mAbs.^{17,18} Here, we brought new data indicating that OAcGD2 mAb-treated cells have increased membrane pores using scanning electron microscopy. More importantly, we demonstrated, here, that the pore formation in the plasma membrane led to a boost of topotecan incorporation in the mAb 8B6-treated tumor cells, based on the measure of intracellular fluorescence of topotecan using flow cytometry. This correlated with a gain of caspase 3-activation, as

evidenced by Western blot analysis. This is the first report indicating that oncosis-like cell death enhances cytotoxic drugs uptake and drug-sensitization in tumor cells. Noteworthy, oncosis has been shown to be caspase 3-independant.³³ This observation contrasts with our Western blot analysis demonstrating the induction of caspase 3-activation upon binding of mAb 8B6 on target tumor cells. However, a recent report suggested that anti-ganglioside mAbs can trigger cell death through multiple mechanisms.³¹ Thus, it is possible that mAb 8B6 induces a bimodal cell death program upon binding to its target antigen on the cell surface. In line with this hypothesis, we showed earlier that the tumor cell death induced by mAb 8B6 was partially caspase 3-dependant.¹² Still to be characterized is the nature of the mechanism that triggers the pore formation induced by mAb to OAcGD2. The available data on the molecular mechanism(s) responsible for the appearance of these pores during oncosis-like cell death induced by mAbs remains fairly unknown.^{17,18} Elucidating these mechanism of action at the molecular level could, however, help to designed more potent combination that would simultaneously target molecular actors involved in the cell death pathway.

Up until now, *in vivo* data using anti-ganglioside mAb combined with anti-cancer cytotoxic drugs are limited.³⁴ In the light of our *in vitro* results demonstrating synergy between mAb 8B6 and topotecan, we sought to determine whether mAb 8B6 would increase the anti-neuroblastoma activity of topotecan under a low-dosage schedule. We found that the addition of mAb 8B6 to topotecan demonstrated potent activity against NXS2 neuroblastoma metastasis in A/J mice and against IMR5 xenografts in immunodeficient NSG mice. These findings corroborate that the anti-tumor effect of topotecan may be enhanced with mAb 8B6 immunotherapy used in a therapeutic scenario. Of note, NSG mice lack both innate and adaptive immunity with loss of B cell, T cell, and NK cell function as well as reduced macrophage and antigen-presenting cell function.³⁵ Thus, immune-mediated mechanisms are not a requirement for the efficacy of the combination therapy. Yet, we need to consider the role of mAb 8B6 Fc portion in enhancing topotecan anti-tumor potency *in vivo*. In addition, immunomodulatory effects of topotecan have been demonstrated in preclinical models at maximal-tolerated dose (MTD).³⁶⁻³⁸ As an unwanted side effect, MTD-chemotherapy also activates the tumor stroma.^{39,40} This activation can promote the growth and survival of residual cancer cells to support recurrence and metastasis.^{39,40} The impact of the stroma on cancer resistance can be, however, tempered by lowering the dosage of chemotherapeutic drug.⁴¹ In agreement with this, low-dose application of topotecan was lately identified as an inducer of a tumor-inhibiting senescence-associated secretory phenotype in neuroblastoma cells.⁴² Furthermore, treatment-associated side effects are likely to be reduced under low-dose drug schedule, as known as metronomic therapy.⁴³ In rapport with this, we studied weight loss as an indicator for systemic tolerability of each tested regimens.²⁵ Our data suggest that the combination regimen was well tolerated, although specific effects in our mouse model cannot predict all patient-observable post antibody infusion effects such as chill, headache, or nausea. Considering the synergistic interactions between mAb 8B6 and topotecan evidenced here, anti-OAcGD2 antibodies could be combined in

clinic with lower than currently used doses of chemotherapy, to try to reduce dose-limiting toxicities. This is particularly exciting, given that the immunomodulatory effects of chemotherapeutic drugs are demonstrated at metronomic dosage.^{44,45} Further studies remain needed to characterize the immune mechanisms, and to elucidate the pharmacodynamic interplay that might be involved in the synergistic interaction between anti-OAcGD2 mAb immunotherapy and topotecan.

To conclude, anti-OAcGD2 mAbs may be applied as an oncosis-inducing reagent to sensitize neuroblastoma cells to cytotoxic anti-cancer drugs. Our findings illuminate further work on clinical evaluation of anti-OAcGD2 mAbs in combination with topotecan, as a novel therapeutic approach to improve survival and/or reduce toxicity of patients with neuroblastoma. In this regard, a recent phase 2 study published during the revision of the present paper, showed that irinotecan-temozolomide in combination with the anti-GD2 antibody dinutuximab is an exciting new therapeutic option for refractory or relapse neuroblastoma.⁴⁶ The irinotecan-temozolomide-dinutuximab treatment improved the 1-year survival rates by 51 points compared to the irinotecan-temozolomide therapy. In this context, elucidation of the potential mechanisms of response that occurs in patients merits consideration.

Material and methods

Antibodies and chemotherapeutic drugs

Anti-OAcGD2 mAb 8B6 (IgG2a, kappa) was obtained previously in our laboratory.⁴⁷ An isotype-control mAb (DOTA-IgG2a, kappa) was used as a negative control. The purity of mAb preparations was verified by SDS-PAGE and size exclusion HPLC analyses as previously described.⁴⁷ Endotoxin quantitation was evaluated using the LAL kinetic chromogenic assay (Lonza, # 50–650U). Topotecan (Hycamtin[®]) was obtained from the pharmacy of the Nantes University Hospital (Nantes, France).

Antibody biotinylation

Monoclonal antibodies were biotinylated using the EZ-Link Sulfo-NHS-LC-Biotinylation kit (ThermoFisher Scientific, # 21327) according to the manufacturer's instructions. One milligram of mAb was dissolved in 1 mL PBS according to the instruction kit. After addition of the Sulfo-NHS-LC-Biotin solution at a molar ratio of 20:1 (biotin:IgG), the reaction mixture was incubated at 4°C (on ice) for 2 hours, and the biotinylated product was purified by gel filtration on a Zeba Desalt Spin Column (provided with the kit). Estimation of biotin incorporation to either mAb 8B6 or anti-DOTA IgG2a mAb was done using HABA (4'-hydroxyazobenzene-2-carboxylic acid, provided with the kit) according to the manufacturer's instructions.

Cell culture

The mouse neuroblastoma NXS2 cell line was a gift from Dr. H. N. Lode (Universitätsklinikum Greifswald, Greifswald, Germany).³⁴ The MYCN-gene amplified human LAN1 and LAN5 neuroblastoma cell lines were obtained from the

Children's Oncology Group Cell Culture and Xenograft Repository (Philadelphia, PA, USA).^{48,49} The MYCN-gene amplified human neuroblastoma IMR5 cell line was generously provided by Dr. Santos Susin (Inserm U.872, Paris, France).⁵⁰ NXS2 cells were authenticated by IDEXX BioResearch

(Ludwigsburg, Germany) and were grown in DMEM (Gibco, # 21969-035) with 10% heat-inactivated fetal calf serum (Gibco, # 10220-106), 2 mM L-Glutamine (Gibco, # 25030-024), 100 units/mL penicillin, and 100 µg/mL streptomycin (Gibco, # 15140-122), at 37°C in 5% CO₂. IMR5, LAN1 and LAN5 cells were authenticated by Eurofins Genomics (Ebersberg, Germany) and were grown in RPMI 1640 (Gibco, #31870-025) with 10% heat-inactivated fetal calf serum (Gibco), 2 mM L-Glutamine (Gibco), 100 units/mL penicillin, and 100 µg/mL streptomycin (Gibco), at 37°C in 5% CO₂. All cell lines were routinely tested for mycoplasma spp.

Cell proliferation analysis

Cell viability was measured using the MTT assay,⁵¹ using the Cell Proliferation Kit I (Roche Diagnostic, # 11465 007 001) according to the manufacturer's instructions. Tumor cells (IMR5: 1 × 10⁴ cells; LAN1: 5 × 10³ cells; LAN5: 1 × 10⁴ cells; NXS2: 5 × 10³ cells) were seeded into 96-well plates in 100 µl of media. The next day, 50 µl (3 times concentrated) of several topotecan and/or mAb 8B6 concentrations prepared in 1:2 serial dilutions were added. After 72 hours, 10 µL of methylthiazole tetrazolium salt stock solution (provided with the kit) were added and incubated at 37°C for 4 hours. Then, 100 µl of solubilization buffer (provided with the kit) were added and the plates incubated for 4 hours at 37°C for color development. Absorbance was recorded at 570 nm against a reference wavelength at 650 nm on a Multiskan reader (Thermo Electron, Waltham, MA, USA). Assays were performed in quadruplicate and experiments were repeated three times. Percentage survival for each dose was calculated by multiplying absorbance values with 100 and divided by control absorbance value. Dose-response curves were analyzed using CompuSyn software (ComboSyn, Inc, Paranus, NJ, USA) to determine the effective dose 50 (ED₅₀) values.

Determination of synergy

Topotecan and mAb 8B6 interactions were analyzed for synergistic, additive, or antagonistic effect using the combination index (CI) method developed by Chou and Talalay.¹⁶ To this end, the effective dose 50 (ED₅₀) for both topotecan and mAb 8B6 were determined prior to experiment set up, as described above. Equipotent ratios of the two compounds were prepared across wide range of concentration and treated the cells in 96-well plate for 72 hours. Percentage survival values were converted into Fa (Fraction affected) values using the formula 1 - (% survival / 100). These values were fed into CompuSyn software (ComboSyn, Inc, Paranus, NJ, USA) to determine combination index values (CI = 1, additivity; CI >1, antagonism; CI <1, synergism) at ED₅₀, ED₇₅ and ED₉₀.

Flow cytometric analysis of O-acetyl GD2 expression

Analysis of cell surface OAcGD2-expression on neuroblastoma cell lines was evaluated by indirect immunofluorescence measured by flow cytometry. We incubated 5×10^5 cells in 96-well microplates with either mAb 8B6 or control antibody at $10 \mu\text{g}/\text{mL}$ for 60 minutes at 4°C in PBS-BSA 1%. Antibody binding was analyzed after reaction with the fluorescein-isothiocyanate conjugated $\text{F}(\text{ab}')_2$ fragment of goat anti-mouse IgG (H+L) as a second antibody (Jackson, Immunoresearch, # 115-096-146) for 60 min at 4°C . Cell fluorescence was analyzed using a FACSCalibur flow cytometer (BD Biosciences, San Jose, CA, USA) and CellQuest Pro software (BD Biosciences). Relative fluorescence intensities of 10,000 cells were recorded as single-parameter histograms (log scale, 1024 channels, and 4 decades) and mean fluorescence intensity (MFI) was calculated for each histogram. Results were expressed as a MFI ratio calculated by dividing the flow cytometric MFI value of cells stained with antigen-specific mAb by the MFI value for the same cells stained with isotype-matched control mAb. This approach allows for comparison of multiple test samples within a group and between different groups.

Scanning electron microscopy

Neuroblastoma cells were incubated with either mAb 8B6 or control antibody for 30 minutes at 37°C , washed three times with PBS, and then fixed with 2% glutaraldehyde (Sigma Aldrich, # G7526) in 0.1 mol/L sodium phosphate buffer (pH = 7.4) at 4°C for one hour. These cells were washed with PBS and post-fixed for 15 minutes in 1% OsO_4 (Sigma Aldrich, # 75633). Then, they were washed three times with PBS, and dehydrated through a graded ethanol (VWR Prolabo, # CHESEA043-2.5LP). Cells were then gold coated for 2 min before analyze by Scanning Electron Microscope (Merlin, Carl Zeiss, Germany). Images were stored as TIFF files with Adobe Photoshop.

Cellular accumulation of topotecan

Topotecan has a UV excitable chromophore. Therefore topotecan uptake into neuroblastoma cells was assayed by flow cytometry using a FACSCalibur flow cytometer (BD Biosciences, San Jose, CA, USA) and CellQuest Pro software (BD Biosciences) as previously described.⁵² Topotecan-derived fluorescence intensity was analyzed in a histogram bi-parametric of the log of orange fluorescence (FL2-H) versus the cell size (FSC-H) after 30 minutes exposure. Mean fluorescence intensity (MFI) was calculated for each histogram. An MFI ratio was calculated by dividing the flow cytometric MFI value of cells incubated with mAb 8B6 plus topotecan by the MFI value for the same cells treated with topotecan alone, and topotecan intracellular accumulation was expressed as fold increase of the MFI ratio of the cell treated with topotecan alone. Parallel samples were incubated with the control antibody as control.

Western blot analysis

Cells (IMR5: 7.5×10^5 cells; LAN1: 5×10^5 cells; LAN5: 8×10^5 cells; NXS2: 8×10^5 cells) were seeded into 6-well culture

plates and treated with mAb 8B6 ($40 \mu\text{g}/\text{mL}$), topotecan (IMR5: 10 nM; LAN1: 800 nM; LAN5: 10 nM; NXS2: 450 nM) and the combination of two drugs for 24 hours. Treated cells were washed twice with ice-cold phosphate-buffered saline, and then lysed using appropriate amount of lysis buffer (20 mM Tris-HCl, pH 7.4, 1% Nonidet P-40, 0.25% DOC, 0.15 M NaCl, 0.1% SDS, 1 mM EDTA, phosphatase and protease inhibitors). Equal amounts of protein ($30 \mu\text{g}$) were separated on SDS-polyacrylamide gel (INVITROGEN, Thermofischer Scientific, #NP0335BOX), and electrotransferred to the polyvinylidene difluoride membrane (PVDF, Millipore, # IPVH00010). Membranes were incubated with 5% milk-phosphate-buffered saline for 1 hour, washed with phosphate-buffered saline containing 0.1% Tween 20, and then incubated with antibodies reactive with cleaved caspase 3 (clone 5A1E, Cell Signaling Technology Inc., # 9664) and β -actin (Clone C4, Merck Millipore, # 6A2910). Secondary horseradish peroxidase-conjugated goat anti-rabbit and monoclonal antibody and goat anti-mouse (Jackson Immunoresearch #115-035-006, #111-035-006) were used for detection of bound primary antibody and bands were visualized by enhanced chemiluminescence (GE Healthcare, # RPN 2236).

Mouse neuroblastoma models

Two neuroblastoma cell lines were used to establish murine tumor models. The mouse NXS2 cell line was used to establish an experimental liver metastasis model in immunocompetent A/J mice, previously described by Lode *et al.*³⁴ The human IMR5 cell line was used to establish subcutaneous xenografts in immunodeficient NSGTM mice.³⁵ All experiments were carried out in strict accordance with the recommendations in the Guide for the Care and Use of Laboratory Animals of the French Department of Agriculture (agreement number: APA-FIS 03479.01). Protocols were approved by the Committee on the Ethics of Animal Experiments of the Région Pays de la Loire (CEEA-PdL 06). Mice were housed at the UTE-UN animal facility (Nantes, France, agreement # C44-278).

Female and male A/J mice (6–8 weeks of age) were obtained from Envigo (Gannat, France, # 4904F). We inoculated 2.5×10^5 tumor cells by tail vein in PBS. We grouped the mice into five groups of 10 mice each: 1) vehicle-treated group; 2) control antibody-treated group; 3) mAb 8B6-treated group; 4) topotecan-treated group; and 5) topotecan + mAb 8B6-treated group. Anti-OAcGD2 mAb 8B6 treatment was started at day 3 after tumor cell injection. Mice received by i.v. injection, twice a week, $25 \mu\text{g}$ mAb for 3 consecutive weeks; (day 3, 7, 10, 14, 17 and 21; total dose = $150 \mu\text{g}$). Topotecan diluted in PBS was given by i.p. injection at $0.36 \text{ mg}/\text{kg}$ daily for 5 consecutive days (days 10–14). Mice were sacrificed after 28 days post inoculation, and anti-tumor efficacy was evaluated by liver weight of the fresh specimen.

Female NSG (7 weeks of age) were obtained from Charles River Laboratories (L'Abresles, France, JAXTM mice strain # 005557). Subcutaneous xenografts were developed by injecting subcutaneously 2.5×10^6 IMR5 cells into the right flank of the mice. Mice with engrafted tumors that reached 50 mm^3 in size were randomized into groups of 10 per condition. Tumors were measured at the initiation of the study and then every

3–4 days using a digital caliper. Tumor volume was calculated using the formula: $(A \times B^2) \times 0.5$ in which A is the largest and B is the shortest dimension. Animals were monitored for body weight and tumor growth. The studies consisted in the same experimental groups as described above. Antibody 8B6 or control antibody treatment (150 $\mu\text{g}/\text{mouse}$) started on day 7 after IMR5 cells inoculation by i.v. injection and was repeated on day 12 (total dose 300 μg). Topotecan treatment started on day 7 following tumor cell inoculation by injecting 0.36 mg/kg topotecan or PBS control i.p. for 5 consecutive days. The event resulting in mouse euthanasia was disease progression, defined as the tumor volume reaching above 1 cm^3 .

Immunohistochemistry on murine neuroblastoma hepatic metastasis samples

OAcGD2 expression was analyzed by an immunoperoxidase assay performed with biotinylated-8B6 mAb on NXS2 neuroblastoma liver metastasis upon mice treatment with topotecan alone as described above. To this purpose, NXS2 tumors grown in A/J treated-mice were embedded in Tissue Tek-II O.C.T. (Sakura, # 4583), snap frozen in isopentane in liquid nitrogen and stored at -80°C . Five micrometer-sections were cut, fixed in acetone and stored at -80°C until use. Tissue sections were blocked with Dako RealTM Peroxidase Block (Dako, # S2023) for 6 minutes and then rinsed with Dako's washing buffer (Dako, # S3306). We then added biotinylated-8B6 mAb onto the sections diluted in Antibody Diluent (Dako, # S3022) at a final concentration of 10 $\mu\text{g}/\text{mL}$ for 1 hour. After rinsing, the bound mAb was detected by incubation with Streptavidin-HRP (Beckman Coulter, # PN IM0309). DAB (Dako, # K3468) was used as HRP substrate and sections were counterstained with hematoxylin (CS700) before immunocytological evaluation. Biotinylated-anti-DOTA mAb was used as a negative control. Slides were imaged with a nanozoomer (Hamamatsu, Hamamatsu City, Japan) and images were stored as TIFF files with Adobe Photoshop. Staining was graded as positive or negative according to the presence or absence of immunoreactivity, respectively.

Statistical analysis

Statistical analysis was performed using Prism software (GraphPad Prism Software). Differences between untreated and treated groups in the *in vitro* experiments were analyzed by two-tailed Student's *t* test. For *in vivo* studies, the statistical significance of either liver weights or tumor volumes of experimental groups of mice was tested by Mann-Whitney test. Event-free survival (EFS) was defined as the percentage of mice that survived while on therapy, where survival was defined as the lack of an "event". We defined an event as a tumor volume reaching above 1 cm^3 , at which point the mice were euthanized and taken off study. EFS percentages were estimated using the Kaplan-Meier method and survival curves were compared using the Log-Rank test. We considered *p* values of less than 0.05 as significant.

Disclosure

Sébastien Faraj, Julien Fleurence, and Stéphane Birklé are designed as inventor of pending patents covering the clinical application of anti-O-acetyl-GD2 therapeutic antibodies.

Acknowledgments

Grant support: *Fondation de Projet de l'Université de Nantes, les Bagouz' à Manon, La Ligue contre le Cancer comité de Loire-Atlantique, comité du Morbihan, and comité de Vendée, une rose pour S.A.R.A.H, l'Etoile de Martin and la Société Française de Lutte contre les Cancers et les leucémies de l'Enfant et de l'adolescent (SFCE)*. We thank CYTOCELL, the MicroPICell-, the P2R protein-, and the UTE-facilities of the *Structure Fédérative de Recherche François Bonamy*, and Denis Cochonneau for technical assistance.

ORCID

S. Birklé  <http://orcid.org/0000-0001-8217-778X>

References

- Nakagawara A, Ohira M. Comprehensive genomics linking between neural development and cancer: neuroblastoma as a model. *Cancer Lett*. 2004;204:213–24. doi:10.1016/S0304-3835(03)00457-9. PMID:15013220
- Katzenstein HM, Bowman LC, Brodeur GM, Thorner PS, Joshi VV, Smith EI, Look AT, Rowe ST, Nash MB, Holbrook T, et al. Prognostic significance of age, MYCN oncogene amplification, tumor cell ploidy, and histology in 110 infants with stage D(S) neuroblastoma: the pediatric oncology group experience—a pediatric oncology group study. *J Clin Oncol*. 1998;16:2007–17. doi:10.1200/JCO.1998.16.6.2007. PMID:9626197
- Cheung NK, Cheung IY, Kushner BH, Ostrovnya I, Chamberlain E, Kramer K, Modak S. Murine anti-GD2 monoclonal antibody 3F8 combined with granulocyte-macrophage colony-stimulating factor and 13-cis-retinoic acid in high-risk patients with stage 4 neuroblastoma in first remission. *J Clin Oncol*. 2012;30:3264–70. doi:10.1200/JCO.2011.41.3807. PMID:22869886
- Mosse YP, Lim MS, Voss SD, Wilner K, Ruffner K, Laliberte J, Rolland D, Balis FM, Maris JM, Weigel BJ, et al. Safety and activity of crizotinib for paediatric patients with refractory solid tumours or anaplastic large-cell lymphoma: a Children's Oncology Group phase 1 consortium study. *Lancet Oncol*. 2013;14:472–80. doi:10.1016/S1470-2045(13)70095-0. PMID:23598171
- Flandin I, Hartmann O, Michon J, Pinkerton R, Coze C, Stephan JL, Fourquet B, Valteau-Couanet D, Bergeron C, Philip T, et al. Impact of TBI on late effects in children treated by megatherapy for Stage IV neuroblastoma. A study of the French Society of Pediatric oncology. *Int J Radiat Oncol Biol Phys*. 2006;64:1424–31. doi:10.1016/j.ijrobp.2005.10.020. PMID:16427213
- Martin A, Schneiderman J, Helenowski IB, Morgan E, Dille K, Danner-Koptik K, Hatahet M, Shimada H, Cohn SL, Kletzel M, et al. Secondary malignant neoplasms after high-dose chemotherapy and autologous stem cell rescue for high-risk neuroblastoma. *Pediatr Blood Cancer*. 2014;61:1350–6. doi:10.1002/pbc.25033. PMID:24634399
- Trahair TN, Vowels MR, Johnston K, Cohn RJ, Russell SJ, Neville KA, Carroll S, Marshall GM. Long-term outcomes in children with high-risk neuroblastoma treated with autologous stem cell transplantation. *Bone Marrow Transplant*. 2007;40:741–6. doi:10.1038/sj.bmt.1705809. PMID:17724446
- Yu AL, Gilman AL, Ozkaynak MF, London WB, Kreissman SG, Chen HX, Smith M, Anderson B, Villablanca JG, Matthay KK, et al. Anti-GD2 antibody with GM-CSF, interleukin-2, and isotretinoin for neuroblastoma. *N Engl J Med*. 2010;363:1324–34. doi:10.1056/NEJMoa0911123. PMID:20879881

9. Yuki N, Yamada M, Tagawa Y, Takahashi H, Handa S. Pathogenesis of the neurotoxicity caused by anti-GD2 antibody therapy. *J Neurol Sci*. 1997;149:127-30. doi:10.1016/S0022-510X(97)05390-2. PMID:9171318
10. Alvarez-Rueda N, Desselle A, Cochonneau D, Chaumette T, Clemencau B, Leprieur S, Bougras G, Supiot S, Mussini JM, Barbet J, et al. A monoclonal antibody to O-acetyl-GD2 ganglioside and not to GD2 shows potent anti-tumor activity without peripheral nervous system cross-reactivity. *PLoS One*. 2011;6:e25220. doi:10.1371/journal.pone.0025220. PMID:21966461
11. Terme M, Dorvillius M, Cochonneau D, Chaumette T, Xiao W, Dicciani MB, Barbet J, Yu AL, Paris F, Sorkin LS, et al. Chimeric antibody c.8B6 to O-acetyl-GD2 mediates the same efficient anti-neuroblastoma effects as therapeutic ch14.18 antibody to GD2 without antibody induced allodynia. *PLoS One*. 2014;9:e87210. doi:10.1371/journal.pone.0087210. PMID:24520328
12. Cochonneau D, Terme M, Michaud A, Dorvillius M, Gautier N, Frickeche J, Alvarez-Rueda N, Bougras G, Aubry J, Paris F, et al. Cell cycle arrest and apoptosis induced by O-acetyl-GD2-specific monoclonal antibody 8B6 inhibits tumor growth in vitro and *in vivo*. *Cancer Lett*. 2013;333:194-204. doi:10.1016/j.canlet.2013.01.032. PMID:23370223
13. Pratt CB, Stewart C, Santana VM, Bowman L, Furman W, Ochs J, Marina N, Kuttesch JF, Heideman R, Sandlund JT, et al. Phase I study of topotecan for pediatric patients with malignant solid tumors. *J Clin Oncol*. 1994;12:539-43. doi:10.1200/JCO.1994.12.3.539. PMID:8120551
14. Hettmer S, McCarter R, Ladisch S, Kaucic K. Alterations in neuroblastoma ganglioside synthesis by induction of GD1b synthase by retinoic acid. *Br J Cancer*. 2004;91:389-97. PMID:15187999
15. Rebhan M, Vacun G, Bayreuther K, Rosner H. Altered ganglioside expression by SH-SY5Y cells upon retinoic acid-induced neuronal differentiation. *Neuroreport*. 1994;5:941-4. doi:10.1097/00001756-199404000-00022. PMID:8061301
16. Chou TC, Talalay P. Quantitative analysis of dose-effect relationships: the combined effects of multiple drugs or enzyme inhibitors. *Adv Enzyme Regul*. 1984;22:27-55. doi:10.1016/0065-2571(84)90007-4. PMID:6382953
17. Roque-Navarro L, Chakrabandhu K, de Leon J, Rodriguez S, Toledo C, Carr A, de Acosta CM, Hueber AO, Perez R. Anti-ganglioside antibody-induced tumor cell death by loss of membrane integrity. *Mol Cancer Ther*. 2008;7:2033-41. doi:10.1158/1535-7163.MCT-08-0222. PMID:18645013
18. Fernandez-Marrero Y, Roque-Navarro L, Hernandez T, Dorvignit D, Molina-Perez M, Gonzalez A, Sosa K, Lopez-Requena A, Perez R, de Acosta CM. A cytotoxic humanized anti-ganglioside antibody produced in a murine cell line defective of N-glycosylated-glycoconjugates. *Immunobiology*. 2011;216:1239-47. doi:10.1016/j.imbio.2011.07.004. PMID:21802167
19. Kane AB. Redefining cell death. *Am J Pathol*. 1995;146:1-2. PMID:7856718
20. Majno G, Joris I. Apoptosis, oncosis, and necrosis. An overview of cell death. *Am J Pathol*. 1995;146:3-15. PMID:7856735
21. Trump BF, Berezsky IK, Chang SH, Phelps PC. The pathways of cell death: oncosis, apoptosis, and necrosis. *Toxicol Pathol*. 1997;25:82-8. doi:10.1177/019262339702500116. PMID:9061857
22. Norris RE, Adamson PC, Nguyen VT, Fox E. Preclinical evaluation of the PARP inhibitor, olaparib, in combination with cytotoxic chemotherapy in pediatric solid tumors. *Pediatr Blood Cancer*. 2014;61:145-50. doi:10.1002/pbc.24697. PMID:24038812
23. Kim ES, Soffer SZ, Huang J, McCrudden KW, Yokoi A, Manley CA, Middleworth W, Kandel JJ, Yamashiro DJ. Distinct response of experimental neuroblastoma to combination antiangiogenic strategies. *J Pediatr Surg*. 2002;37:518-22. doi:10.1053/jpsu.2002.30855. PMID:11877680
24. Iyer R, Evans AE, Qi X, Ho R, Minturn JE, Zhao H, Balamuth N, Maris JM, Brodeur GM. Lestaurtinib enhances the antitumor efficacy of chemotherapy in murine xenograft models of neuroblastoma. *Clin Cancer Res*. 2010;16:1478-85. doi:10.1158/1078-0432.CCR-09-1531. PMID:20179224
25. Ullman-Cullere MH, Foltz CJ. Body condition scoring: a rapid and accurate method for assessing health status in mice. *Lab Anim Sci*. 1999;49:319-23. PMID:10403450
26. Morgenstern DA, Baruchel S, Irwin MS. Current and future strategies for relapsed neuroblastoma: challenges on the road to precision therapy. *J Pediatr Hematol Oncol*. 2013;35:337-47. doi:10.1097/MPH.0b013e318299d637. PMID:23703550
27. Kowalczyk A, Gil M, Horwacik I, Odrowaz Z, Kozbor D, Rokita H. The GD2-specific 14G2a monoclonal antibody induces apoptosis and enhances cytotoxicity of chemotherapeutic drugs in IMR-32 human neuroblastoma cells. *Cancer Lett*. 2009;281:171-82. doi:10.1016/j.canlet.2009.02.040. PMID:19339105
28. Yoshida S, Fukumoto S, Kawaguchi H, Sato S, Ueda R, Furukawa K. Ganglioside G(D2) in small cell lung cancer cell lines: enhancement of cell proliferation and mediation of apoptosis. *Cancer Res*. 2001;61:4244-52. PMID:11358851
29. Sjoberg ER, Manzi AE, Khoo KH, Dell A, Varki A. Structural and immunological characterization of O-acetylated GD2. Evidence that GD2 is an acceptor for ganglioside O-acetyltransferase in human melanoma cells. *J Biol Chem*. 1992;267:16200-11. PMID:1644805
30. Ye JN, Cheung NK. A novel O-acetylated ganglioside detected by anti-GD2 monoclonal antibodies. *Int J Cancer*. 1992;50:197-201. doi:10.1002/ijc.2910500207. PMID:1730513
31. Tsao CY, Sabbatino F, Cheung NV, Hsu JC, Villani V, Wang X, Ferrone S. Anti-proliferative and pro-apoptotic activity of GD2 ganglioside-specific monoclonal antibody 3F8 in human melanoma cells. *Oncoimmunology*. 2015;4:e1023975. doi:10.1080/2162402X.2015.1023975. PMID:26405581
32. Goto S, Umehara S, Gerbing RB, Stram DO, Brodeur GM, Seeger RC, Lukens JN, Matthay KK, Shimada H. Histopathology (International Neuroblastoma Pathology Classification) and MYCN status in patients with peripheral neuroblastic tumors: a report from the Children's Cancer Group. *Cancer*. 2001;92:2699-708. doi:10.1002/1097-0142(20011115)92:10%3c2699::AID-CNCR1624%3e3.0.CO;2-A. PMID:11745206
33. Weerasinghe P, Hallock S, Tang SC, Liepins A. Sanguinarine induces bimodal cell death in K562 but not in high Bcl-2-expressing JM1 cells. *Pathol Res Pract*. 2001;197:717-26. doi:10.1078/0344-0338-00150. PMID:11770015
34. Lode HN, Xiang R, Varki NM, Dolman CS, Gillies SD, Reisfeld RA. Targeted interleukin-2 therapy for spontaneous neuroblastoma metastases to bone marrow. *J Natl Cancer Inst*. 1997;89:1586-94. doi:10.1093/jnci/89.21.1586. PMID:9362156
35. Ishikawa F, Yasukawa M, Lyons B, Yoshida S, Miyamoto T, Yoshimoto G, Watanabe T, Akashi K, Shultz LD, Harada M. Development of functional human blood and immune systems in NOD/SCID/IL2 receptor {gamma} chain(null) mice. *Blood*. 2005;106:1565-73. doi:10.1182/blood-2005-02-0516. PMID:15920010
36. Wei J, DeAngulo G, Sun W, Hussain SF, Vasquez H, Jordan J, Weinberg J, Wolff J, Koshkina N, Heimberger AB. Topotecan enhances immune clearance of gliomas. *Cancer Immunol Immunother*. 2009;58:259-70. doi:10.1007/s00262-008-0550-1. PMID:18594817
37. Trojandt S, Knies D, Pektor S, Ritz S, Mailander V, Grabbe S, Reske-Kunz AB, Bros M. The chemotherapeutic agent topotecan differentially modulates the phenotype and function of dendritic cells. *Cancer Immunol Immunother*. 2013;62:1315-26. doi:10.1007/s00262-013-1431-9. PMID:23666509
38. Kitai Y, Kawasaki T, Sueyoshi T, Kobiyama K, Ishii KJ, Zou J, Akira S, Matsuda T, Kawai T. DNA-Containing Exosomes Derived from Cancer Cells Treated with Topotecan Activate a STING-Dependent Pathway and Reinforce Antitumor Immunity. *J Immunol*. 2017;198:1649-59. doi:10.4049/jimmunol.1601694. PMID:28069806
39. Sonnenberg M, van der Kuip H, Haubeis S, Fritz P, Schroth W, Friedel G, Simon W, Murdter TE, Aulitzky WE. Highly variable response to cytotoxic chemotherapy in carcinoma-associated fibroblasts (CAFs) from lung and breast. *BMC Cancer*. 2008;8:364. doi:10.1186/1471-2407-8-364. PMID:19077243
40. Daenen LG, Roodhart JM, van Amersfoort M, Dehnad M, Roessingh W, Ulfman LH, Derksen PW, Voest EE. Chemotherapy enhances metastasis formation via VEGFR-1-expressing endothelial cells. *Cancer Res*. 2011;71:6976-85. doi:10.1158/0008-5472.CAN-11-0627. PMID:21975929
41. Chan TS, Hsu CC, Pai VC, Liao WY, Huang SS, Tan KT, Yen CJ, Hsu SC, Chen WY, Shan YS, et al. Metronomic chemotherapy prevents therapy-induced stromal activation and induction of tumor-initiating cells. *J Exp Med*. 2016;213:2967-88. doi:10.1084/jem.20151665. PMID:27881732

42. Taschner-Mandl S, Schwarz M, Blaha J, Kauer M, Kromp F, Frank N, Rifatbegovic F, Weiss T, Ladenstein R, Hohenegger M, et al. Metronomic topotecan impedes tumor growth of MYCN-amplified neuroblastoma cells *in vitro* and *in vivo* by therapy induced senescence. *Oncotarget*. 2016;7:3571-86. doi:10.18632/oncotarget.6527. PMID:26657295
43. Hanahan D, Bergers G, Bergsland E. Less is more, regularly: metronomic dosing of cytotoxic drugs can target tumor angiogenesis in mice. *J Clin Invest*. 2000;105:1045-7. doi:10.1172/JCI9872. PMID:10772648
44. Nars MS, Kaneno R. Immunomodulatory effects of low dose chemotherapy and perspectives of its combination with immunotherapy. *Int J Cancer*. 2013;132:2471-8. doi:10.1002/ijc.27801. PMID:22927096
45. Kareva I, Waxman DJ, Lakka Klement G. Metronomic chemotherapy: an attractive alternative to maximum tolerated dose therapy that can activate anti-tumor immunity and minimize therapeutic resistance. *Cancer Lett*. 2015;358:100-6. doi:10.1016/j.canlet.2014.12.039. PMID:25541061
46. Mody R, Naranjo A, Van Ryn C, Yu AL, London WB, Shulkin BL, Parisi MT, Servaes SE, Diccianni MB, Sondel PM, et al. Irinotecan-temozolomide with temsirolimus or dinutuximab in children with refractory or relapsed neuroblastoma (COG ANBL1221): an open-label, randomised, phase 2 trial. *Lancet Oncol*. 2017;18:946-57. doi:10.1016/S1470-2045(17)30355-8. PMID:28549783
47. Fleurence J, Cochonneau D, Fougerey S, Oliver L, Geraldo F, Terme M, Dorvillius M, Loussouarn D, Vallette F, Paris F, et al. Targeting and killing glioblastoma with monoclonal antibody to O-acetyl GD2 ganglioside. *Oncotarget*. 2016;7:41172-85. doi:10.18632/oncotarget.9226. PMID:27172791
48. Huang R, Cheung NK, Vider J, Cheung IY, Gerald WL, Tickoo SK, Holland EC, Blasberg RG. MYCN and MYC regulate tumor proliferation and tumorigenesis directly through BMI1 in human neuroblastomas. *FASEB J*. 2011;25:4138-49. doi:10.1096/fj.11-185033. PMID:21856782
49. Foley NH, Bray I, Watters KM, Das S, Bryan K, Bernas T, Prehn JH, Stallings RL. MicroRNAs 10a and 10b are potent inducers of neuroblastoma cell differentiation through targeting of nuclear receptor corepressor 2. *Cell Death Differ*. 2011;18:1089-98. doi:10.1038/cdd.2010.172. PMID:21212796
50. Fischer M, Berthold F. Characterization of the gene expression profile of neuroblastoma cell line IMR-5 using serial analysis of gene expression. *Cancer Lett*. 2003;190:79-87. doi:10.1016/S0304-3835(02)00581-5. PMID:12536080
51. Denizot F, Lang R. Rapid colorimetric assay for cell growth and survival. Modifications to the tetrazolium dye procedure giving improved sensitivity and reliability. *J Immunol Methods*. 1986;89:271-7. doi:10.1016/0022-1759(86)90368-6. PMID:3486233
52. Kawabata S, Oka M, Soda H, Shiozawa K, Nakatomi K, Tsurutani J, Nakamura Y, Doi S, Kitazaki T, Sugahara K, et al. Expression and functional analyses of breast cancer resistance protein in lung cancer. *Clin Cancer Res*. 2003;9:3052-7. PMID:12912956
53. Ushmorov A, Debatin KM, Beltinger C. Growth inhibition of murine neuroblastoma cells by c-myc with cell cycle arrest in G2/M. *Cancer Biol Ther*. 2005;4:181-6. doi:10.4161/cbt.4.2.1439. PMID:15684616
54. Gilbert F, Balaban G, Moorhead P, Bianchi D, Schlesinger H. Abnormalities of chromosome 1p in human neuroblastoma tumors and cell lines. *Cancer Genet Cytogenet*. 1982;7:33-42. doi:10.1016/0165-4608(82)90105-4. PMID:7139592
55. Brodeur GM, Green AA, Hayes FA, Williams KJ, Williams DL, Tsatis AA. Cytogenetic features of human neuroblastomas and cell lines. *Cancer Res*. 1981;41:4678-86. PMID:6171342
56. Ribatti D, Raffaghello L, Pastorino F, Nico B, Brignole C, Vacca A, Ponzoni M. *In vivo* angiogenic activity of neuroblastoma correlates with MYCN oncogene overexpression. *Int J Cancer*. 2002;102:351-4. doi:10.1002/ijc.10742. PMID:12402304